PHYSICAL REVIEW B **71**, 081403(R) (2005)

Supported nanoclusters: Preadsorbates tuning catalytic activity

Ž. Šljivančanin and Alfredo Pasquarello
Institut de Théorie des Phénomènes Physiques (ITP), Ecole Polytechnique Fédérale de Lausanne (EPFL), CH-1015 Lausanne, Switzerland
and Institut Romand de Recherche Numérique en Physique des Matériaux (IRRMA), CH-1015 Lausanne, Switzerland
(Received 4 November 2004; published 23 February 2005)

Using a density-functional approach, we investigate the reactivity of supported metal nanoclusters. We focus on the sequential adsorption of N_2 molecules on a Fe nanocluster supported by an MgO substrate. For an increasing number of N atoms preadsorbed on the nanocluster, we found that the binding energy of the N_2 molecule increases, and can become higher than that of its dissociation products, in marked contrast with the behavior at the respective metallic surface. We identify the electrostatic interaction as a primary factor determining this behavior, and discuss the observed trends in terms of interactions with highest occupied and lowest unoccupied molecular orbitals.

DOI: 10.1103/PhysRevB.71.081403 PACS number(s): 68.35.Dv, 82.20.Kh, 82.30.Lp, 82.65.+r

Following the observation of the surprisingly enhanced reactivity of gold nanoclusters with respect to the inert gold surfaces, the catalytic properties of nanosize particles have recently attracted a great deal of attention.[1–4] Considerable efforts are being sustained towards the design of nanoclusters with specific catalytic functionalities.[5–7] Understanding the mechanisms affecting the catalytic properties of nanoclusters would contribute to guiding those efforts. However, most of the progress has so far been obtained empirically.

In this work, we set out to identifying the relevant factors determining the reactivity of nanosize catalysts, using a density-functional approach. We focused on the reaction of N_2 molecules with a supported Fe nanocluster, because of the importance of nitrogen fixation in industrial[8,9] and biological[10–12] processes. We describe catalytic properties by calculating binding energies of atomic and molecular nitrogen and by evaluating the dissociation barriers of adsorbed N_2 molecules. We highlight the role of preadsorbates in affecting the cluster reactivity, showing that they can stabilize adsorbed N_2 molecules and quench their dissociation. Such a stabilization opens the way to reaction pathways involving the N_2 molecule as an intermediate state.[13] Hence, nanoclusters with preadsorbates may carry catalytic functionalities differing significantly from both the pristine clusters and the relative metallic surfaces, where the N_2 molecule immediately dissociates upon adsorption.

As model catalysts, we focused on Fe_7 clusters deposited on a MgO(100) substrate. Metal clusters of similar size have been shown to carry peculiar electronic properties, quite distinct with respect to those of competetive metallic surfaces.[6] We chose MgO as an inert substrate, often used in experimental setups. We used a supercell slab geometry in which the MgO surface was modeled by two layers[14] with 18 atoms per layer, separated by 13 Å of vacuum. The structure of the Fe_7/MgO cluster prior to N absorption was taken from Ref. 15.

We described the electronic structure within a spin-dependent generalized gradient approximation[16] to density-functional theory. Only valence wave functions were treated explicitly and valence core interactions were described by ultrasoft pseudopotentials.[17–20] The electron wave functions and the augmented electron density were expanded in plane waves with cutoff energies of 25 and 140 Ry, respectively. We obtained converged energies using a Brillouin-zone sampling of 4 **k** points.[21] The positions of the atoms were always relaxed, except those of the bottom MgO layer which were held in ideal bulk positions. Dissociation barriers were calculated through geometry optimizations with fixed N-N bond length varying between 1.6 and 2.2 Å with increments of 0.2 Å. The nitrogen adsorption energies are referred to half the energy of a gas-phase N_2 molecule.

Atomic nitrogen. We studied the adsorption of atomic nitrogen on the Fe_7/MgO cluster by performing a set of calculations in which the number of adsorbates is varied from one to six. For a given number of adsorbed N atoms, we examined different adsorption sites and cluster geometries and reported results for the configuration with the lowest total energy. We investigated N locations outside and inside the bare Fe_7/MgO cluster, as well as completely different morphologies inspired from crystalline iron nitride.[22] The first adsorbed N atom occupies a threefold hollow site, as shown in Fig. 1(i). We found a binding energy of 0.88 eV for this geometry. The second N atom adsorbs in a nearby threefold site [see Fig. 1(ii)]. In this configuration, one of the Fe atoms of the cluster forms bonds with both adsorbed N atoms. The potential energy of the Fe_7/MgO cluster with two chemisorbed N atoms decreases to −2.09 eV. The most favorable adsorption geometry for three N atoms interacting with the cluster corresponds to a stable triangular structure, shown in Fig. 1(iii). The potential energy of this configuration is −2.99 eV. The adsorption geometries for four and five adsorbed N atoms are shown in Figs. 1(iv) and 1(v), respectively. In both these configurations, the cluster undergoes a deformation which gives rise to a fourfold hollow site, where one of the N atoms can bind in a particularly strong way.[23] The other N atoms then occupy available threefold hollow sites. We calculated potential energies of −3.91 and −5.10 eV for four and five adsorbed N atoms, respectively. When a sixth N atom is brought to interact with the cluster, we found that the most favorable configuration shows this atom on top of an Fe atom [Fig. 1(vi)]. For this geometry, we obtained a potential energy of −4.42 eV, higher than for the

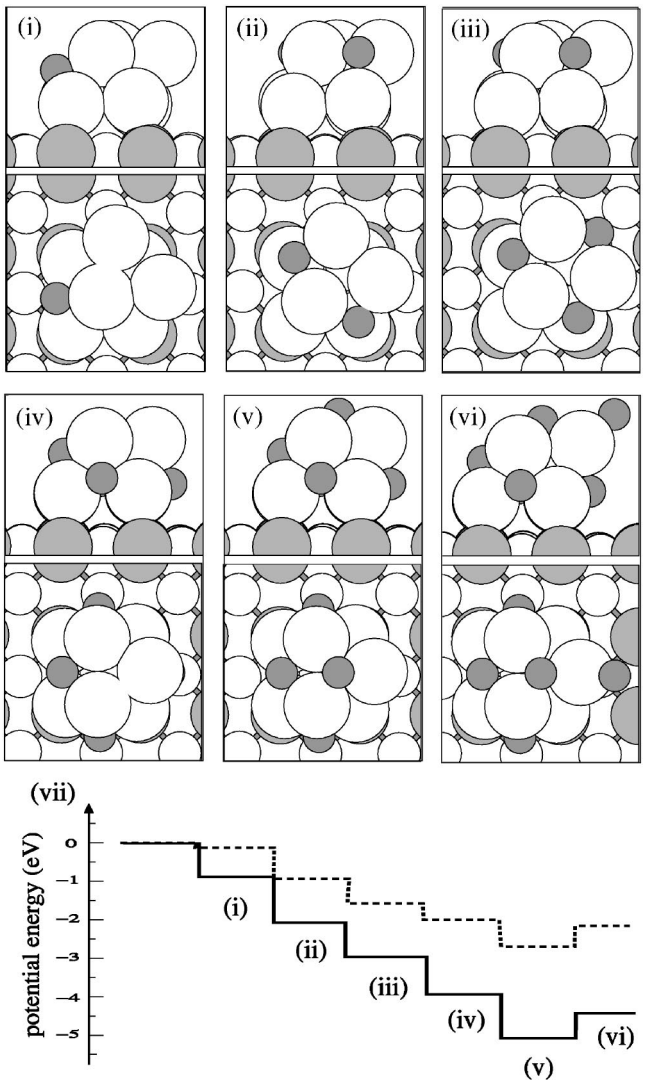

FIG. 1. Side and top views of the adsorption geometries for *n* N atoms on the Fe_7/MgO cluster, with *n* varying from (i) one to (vi) six. Balls represent Fe (large white), O (dark gray), Mg (small white), and N atoms (dark gray). (vii) Corresponding potential-energy diagram: with (solid) and without (dashed) the MgO support.

Fe_7/MgO cluster with five adsorbed N atoms [Fig. 1(v)]. The increase of the potential energy results from the strong repulsive effect due to nearby preadsorbed N atoms. The dependence of the potential energies on the number of N adsorbates is shown in Fig. 1(vii).

Molecular nitrogen. We studied the sequential adsorption of three N_2 molecules on the Fe_7/MgO cluster. At every step, we searched for the most favorable geometries. The corresponding adsorption geometries and potential energies are given in Fig. 2. The first N_2 molecule adsorbs in an end-on geometry [labeled I in Fig. 2(a)] with a binding energy of 0.81 eV. From this adsorption geometry, the molecule can move to another configuration showing two contact points to the cluster [labeled II in Fig. 2(a)], higher in energy by 0.29 eV. However, the geometry with two contact points is essential for a dissociation with a small activation energy. The

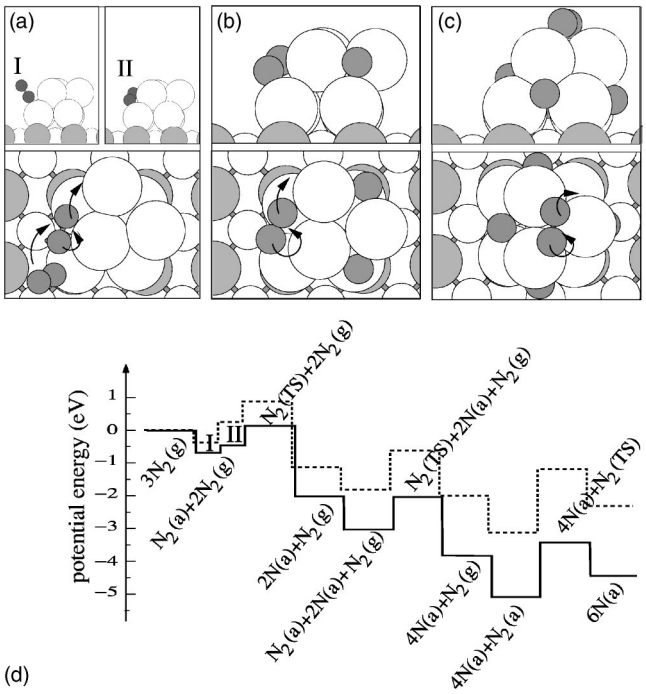

FIG. 2. Side and top views of the N_2 molecule on the Fe_7/MgO cluster with (a) no, (b) two, and (c) four preadsorbed N atoms. (d) Potential-energy diagram for the sequential dissociation of N_2 molecules on the Fe_7 cluster: with (solid) and without (dashed) the MgO support.

potential energy of the N_2 molecule at the transition state is only 0.1 eV higher than in the gas phase. The released N atoms bind strongly to the cluster [Fig. 1(ii)], lowering the potential energy of the system to −2.09 eV. The second N_2 molecule adsorbs on the Fe_7/MgO cluster in the configuration shown in Fig. 2(b), with a binding energy of 0.95 eV. The dissociation requires an energy of 0.97 eV. At the transition state, the potential energy is higher than in the gas phase by only 0.02 eV. The final-state configuration is shown in Fig. 1(iv). The third N_2 molecule binds on top of the cluster with four preadsorbed N atoms [see Fig. 2(c)]. The binding energy has increased to 1.25 eV, suggesting a strong attractive interaction between the N_2 molecule and the preadsorbates. For the dissociation of this third N_2 molecule, we calculated an energy barrier of 1.74 eV, corresponding to a potential energy at the transition state higher by 0.49 eV than in the gas phase. The resulting configuration with six adsorbed N atoms [Fig. 1(vi)] is higher in energy by 0.74 eV with respect to the molecular adsorbed state [Fig. 2(c)]. The stability of the molecular state against dissociation opens the possibility for a distinctive catalytic activity at the nanocluster. The preadsorbates contribute to achieving this effect in two ways: (i) by enhancing the binding of the third N_2 molecule, and (ii) by weakening the binding of six adsorbed N atoms. A similar formation of the molecular species has previously been reported for hydrogen at stepped metal surfaces.[24,25] However, the molecular species was not found in a thermodynamically stable state as in the present study.

The support has been recognized for affecting the catalytic properties of deposited clusters.[2,4,26–28] To estimate this

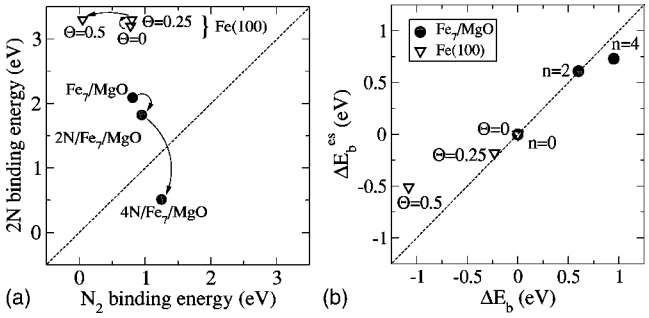

FIG. 3. (a) Comparison between the binding energies of two N atoms and of the N_2 molecule at Fe(100) surfaces (triangles) and on the Fe_7/MgO clusters (circles). The arrows indicate the evolution for an increasing number of preadsorbates. (b) Variations of the N_2 electrostatic binding energy (ΔE_b^{es}) upon removal of preadsorbed N atoms vs corresponding variations of the full binding energy (ΔE_b), for different coverages Θ at the surface and different number n of N preadsorbates on the cluster.

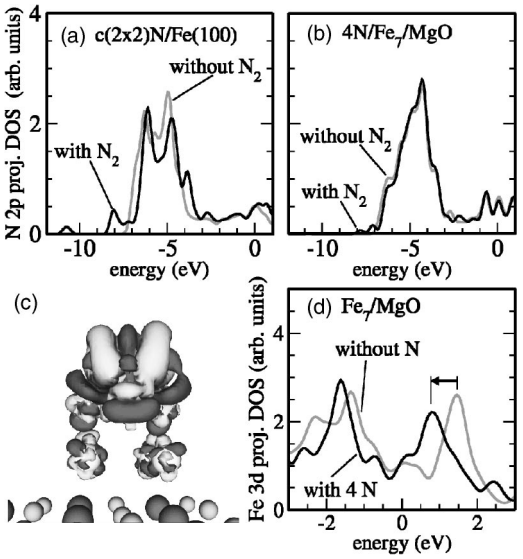

FIG. 4. Electron density of states (DOS) projected on N $2p$ states for (a) the $c(2\times2)N/Fe(100)$ surface and (b) the Fe_7/MgO cluster, before (black) and after (gray) N_2 adsorption. (c) Induced electron density upon N_2 adsorption at the Fe_7/MgO, showing electron accumulation (light gray) and depletion (dark gray). (d) Electron DOS projected on $3d$ states of Fe atoms in direct contact with the N_2 molecule for the Fe_7/MgO cluster, with (black) and without (gray) preadsorbed N atoms.

effect on the binding of N atoms and N_2 molecules to the Fe_7/MgO cluster, we calculated total energies for the structures in Figs. 1 and 2 in the absence of the substrate, without allowing for further atomic relaxation. The results are shown in Figs. 1(vii) and 2(d)(dashed lines). Overall, the substrate increases the binding by about 0.4 eV per N atom. Monitoring the variation of the density of states projected on the Fe $3d$ orbitals, we infer the following picture for this enhanced stability. The interaction between the cluster and the substrate destabilizes the electrons close to the Fermi level, as a result of the formation of antibonding states of primarily Fe $3d$ character derived from Fe $3d$ and O $2p$ orbitals. Upon interaction with a N atom, the electrons in these states are transferred to more favorable bonding states involving N $2p$ and Fe $3d$ orbitals. Because of the destabilization due to the support, the energy gain is larger than in the absence of support.

It is interesting to draw a comparison with the Fe(100) surface. For this surface, we calculated a binding energy of about 1.6 eV per N atom, noticeably higher than the average binding energy of 1.1 eV per N atom at the Fe_7/MgO cluster. This difference is caused by the energetically convenient fourfold hollow sites,[23] which occur at the surface but are absent on the cluster prior to N adsorption. For the N_2 molecule, we found similar adsorption energies on the Fe(100) surface and on the Fe_7/MgO cluster in the absence of preadsorbed N atoms [Fig. 3(a)]. When the coverage of preadsorbed N atoms at the Fe(100) surface is increased up to half a monolayer, the N_2 binding energy is found to *decrease*. On the contrary, at the Fe_7/MgO cluster, the N_2 binding energy *increases* with the number of preadsorbed N atoms.

To understand this complex binding behavior of the N_2 molecule, we consider the electrostatic energy:

$$E^{es} = \frac{1}{2}\int\int \frac{\rho(\mathbf{r})\rho(\mathbf{r}')}{|\mathbf{r}-\mathbf{r}'|} d\mathbf{r}d\mathbf{r}', \qquad (1)$$

where $\rho(\mathbf{r})$ comprises both the electronic and the ionic charges in our calculation. We derived the electrostatic binding energy from differences of electrostatic energies, in the same way as the binding energy is obtained from differences of total energies. For both the Fe(100) surfaces and the Fe_7/MgO clusters, we focus on variations of the electrostatic binding energies upon removal of the preadsorbed N atoms. Figure 3(b) shows that these variations account for a large fraction of the corresponding variations of binding energies obtained from total energies. At the clusters, the electrostatic energy is seen to enhance the binding energy for an increasing number of preadsorbates, while the opposite trend is observed at the surfaces. This behavior is consistent with the fact that the distance between preadsorbed and molecular N atoms on the cluster is larger by 0.6 Å than at the surface. Hence, the binding of molecular nitrogen is favored by electrostatically convenient arrangements of preadsorbates, which can be achieved on the three-dimensional nanoclusters but not on flat surfaces.

The binding behavior of the N_2 molecule can also be analyzed in terms of the interaction of the 5σ [highest occupied molecular orbital (HOMO)] and the 2π [lowest unoccupied molecular orbital (LUMO)] molecular orbitals. Upon adsorption, the 5σ molecular orbital, lower than the Fermi energy by 6 eV, gives rise to a *repulsive* interaction between filled states.[29] In Figs. 4(a) and 4(b), we show how the electronic density of states (DOS) projected on the $2p$ states of the preadsorbed N atoms changes upon N_2 adsorption for two cases. At the $c(2\times2)N/Fe(100)$ surface [Fig. 4(a)], the interaction gives rise to states split off from the main N $2p$ band and to an overall shift of 0.1 eV to higher energies. The occurrence of this repulsive interaction is consistent with the decrease of the N_2 binding energy found at the Fe(100) surface for increasing N coverage. At the Fe_7/MgO cluster [Fig.

4(b)], the N 2*p* band shows only small changes, indicating that this repulsive interaction plays a minor role in this case.

By contrast, the interaction between the Fe 3*d* states and the molecular 2π orbital (LUMO) is *attractive*.[30] Prior to interaction, the energy level of the molecular 2π orbital is higher than the Fermi level by about 1.5 eV. Hence, the interaction primarily involves the empty Fe 3*d* states in the vicinity of the Fermi level, which are predominantly of spin-minority character. Upon interaction with the molecular 2π orbital, the bonding combinations with the latter states can be pushed below the Fermi level and contribute in this way to enhancing the binding energy. To illustrate this mechanism, we plot in Fig. 4(c) the induced electron density for the Fe_7/MgO cluster, obtained as a difference between the cases of an interacting and a noninteracting N_2 molecule. From the shape of the distribution, one recognizes that electron charge accumulates in the molecular 2π orbital. In the presence of preadsorbed N atoms, the overall shape of this distribution does not change (not shown), but the amount of charge transferred to the molecular 2π orbital increases with the number of preadsorbed N atoms. The preadsorbed N atoms cause a reduction of the exchange splitting of the Fe 3*d* states, and consequently a shift of the spin-minority Fe 3*d* levels to lower energies. The latter effect is clearly observed in Fig. 4(d), where the electron DOS projected on the interacting Fe 3*d* states are compared for the Fe_7/MgO cluster with and without preadsorbed N atoms. For the Fe_7/MgO cluster with preadsorbed N atoms, the shift of the empty Fe 3*d* states to energies closer to the Fermi level favors their occupation upon interaction with the molecular 2π orbitals, resulting in an increase of the N_2 binding energy.

In conclusion, focusing on the interaction with molecular nitrogen, we showed that metal nanoclusters can exhibit catalytic properties qualitatively different from their respective surfaces. Our work shows that the electrostatic interaction plays a primary role in affecting the cluster reactivity and implies that its functionality can be tuned by controlling the location of preadsorbates on the nanocluster. Insofar as nanoclusters offer a larger variety of adsorption sites than surfaces, this tunability should be considered as a truly nano-specific property of supported metal clusters.

We thank H. Brune for fruitful interactions. The calculations were performed at the central computational facilities of the Ecole Polytechnique Fédérale de Lausanne and of the Swiss Center for Scientific Computing.

[1] M. Haruta, Catal. Today **36**, 153 (1997).
[2] M. Valden, X. Lai, and D. W. Goodman, Science **281**, 1647 (1998).
[3] A. Sanchez, S. Abbet, U. Heiz, W.-D. Schneider, H. Hakkinen, R. Bernett, and U. Landman, J. Phys. Chem. A **103**, 9573 (1999).
[4] L. M. Molina and B. Hammer, Phys. Rev. Lett. **90**, 206102 (2003).
[5] A. S. Wörz, K. Judai, S. Abbet, and U. Heiz, J. Am. Chem. Soc. **125**, 7964 (2003).
[6] B. C. Gates, Chem. Rev. (Washington, D.C.) **95**, 511 (1995).
[7] U. Heiz and W.-D. Schneider, in *Metal Clusters at Surfaces*, edited by K.-H. Meiwes-Broer (Springer, Heidelberg, 2000).
[8] G. Ertl, and H. J. Freund, Phys. Today **52**, 32 (1999).
[9] K. W. Kolasinski, *Surface Science: Foundations of Catalysis and Nanoscience* (Wiley, New York, 2002).
[10] L. Stryer, *Biochemistry*, 4th ed. (Freeman, New York, 1995).
[11] B. K. Burges and D. J. Lowe, Chem. Rev. (Washington, D.C.) **96**, 2983 (1996).
[12] T. H. Rod, B. Hammer, and J. K. Nørskov, Phys. Rev. Lett. **82**, 4054 (1999).
[13] T. H. Rod and J. K. Nørskov, Surf. Sci. **500**, 678 (2002); T. H. Rod, A. Logadottir, and J. K. Nørskov, J. Chem. Phys. **112**, 5343 (2000).
[14] Test calculations with a third layer gave adsorption energies differing by less than 0.03 eV per adsorbed N atom.
[15] Ž. Šljivančanin and A. Pasquarello, Phys. Rev. Lett. **90**, 247202 (2003).
[16] J. P. Perdew, J. A. Chevary, S. H. Vosko, K. A. Jackson, M. R. Pederson, D. J. Singh, and C. Fiolhais, Phys. Rev. B **46**, 6671 (1992).
[17] D. Vanderbilt, Phys. Rev. B **41**, R7892 (1990).
[18] A. Pasquarello, K. Laasonen, R. Car, C. Lee, and D. Vanderbilt, Phys. Rev. Lett. **69**, 1982 (1992).
[19] K. Laasonen, A. Pasquarello, R. Car, C. Lee, and D. Vanderbilt, Phys. Rev. B **47**, 10 142 (1993).
[20] We used the computer code DACAPO developed by B. Hammer *et al.* See http://www.fysik.dtu.dk/CAMPOS/
[21] H. J. Monkhorst and J. D. Pack, Phys. Rev. B **13**, 5188 (1976).
[22] K. Suzuki, H. Morite, T. Kaneko, H. Yoshida, and H. Fujimori, J. Alloys Compd. **201**, 11 (1993).
[23] J. J. Mortensen, L. B. Hansen, B. Hammer, and J. K. Nørskov, J. Catal. **182**, 479 (1999).
[24] A.-S. Mårtensson, Surf. Sci. **215**, 55 (1989).
[25] P. K. Schmidt, K. Christmann, G. Kresse, J. Hafner, M. Lischka, and A. Gross, Phys. Rev. Lett. **87**, 096103 (2001).
[26] G. A. Somorjai, Surf. Sci. **299-300**, 849 (1994).
[27] K. Hayek, R. Kramer, and Z. Paál, Appl. Catal., A **162**, 1 (1997).
[28] B. Hammer, Phys. Rev. Lett. **89**, 016102 (2002).
[29] R. Hoffmann, Rev. Mod. Phys. **60**, 601 (1988).
[30] B. Hammer and J. K. Nørskov, Adv. Catal. **45**, 71 (2000).